

Electrical properties of Cd-doped and Mg-doped InP

M. Benzaquen and B. Belache

Physics Department, McGill University, 3600 University Street, Montréal, Québec, Canada H3A 2T8

C. Blaauw

Bell-Northern Research Ltd., P.O. Box 3511, Station C, Ottawa, Ontario, Canada K1Y 4H7

(Received 23 January 1992)

We report on Hall transport measurements of two *p*-type Cd-doped InP epilayers and two Mg-doped InP layers with low compensation levels. The acceptor concentrations and the compensation ratios were determined with an extended-state Hall transport model, which provided a good description of the mobilities and the free-hole concentrations. Binding energies of 51 and 38.7 meV were measured for the purest Cd- and Mg-doped samples, respectively. Nearest-neighbor hopping was present in all samples, consistent with a model by Shklovskii and Efros. Saturation of the corresponding conductivity was observed in the Mg-doped samples, in excellent agreement with a model by Shklovskii and Yanchev. Variable-range hopping was observed below 6 K, and was found to be consistent with Mott's expression for the conductivity. An unusual sign reversal of the Hall constant was observed in the Mg-doped samples at the onset of impurity conduction.

I. INTRODUCTION

We have recently reported on the results of temperature-dependent Hall transport measurements¹ for several InP epilayers, grown by metal-organic chemical-vapor deposition (MOCVD) on semi-insulating Fe-doped InP substrates, using Zn as a *p*-type dopant at levels in the range of 7×10^{16} to 2×10^{18} cm⁻³. Nearest-neighbor hopping was observed in all samples, and found to be consistent with a theory by Shklovskii and Efros.² In the purest epilayers, saturation of the nearest-neighbor hopping conductivity was observed, which appeared to be in qualitative agreement with a theory by Shklovskii and Yanchev.³ At sufficiently low temperatures, the electrical conduction in all samples was by means of variable-range hopping. Mott's expression for the conductivity provided an excellent description of the experimental data, and good agreement was obtained between theory and experiment for the activation energies.

In this paper, we extend those transport measurements to *p*-type InP samples in which either Cd or Mg, rather than Zn, is the acceptor species.

II. EXPERIMENT

Epitaxial layers of InP were grown by MOCVD on semi-insulating Fe-InP substrates. In earlier publications, we have discussed the growth and characterization of InP layers doped with Cd (Ref. 4) or Mg.⁵

Meaningful analysis of Hall transport measurements requires a uniform dopant concentration in the layers. This requirement was met in the case of InP layers doped with Cd, where the as-grown layers could be directly used for Hall transport measurements (Cd-doped sample Nos. 1 and 2). However, in the case of Mg doping, poor control of the dopant incorporation process resulted in nonuniform Mg depth concentration profiles in the layers, which rendered the as-grown layers unsuitable for

the Hall transport measurements. Nevertheless, the diffusion characteristics of Mg in InP made it possible to fabricate layers of InP uniformly doped with Mg.

During the growth of Mg-doped InP layers at high-Mg doping levels, significant diffusion of Mg into the substrates took place.⁵ As discussed in earlier work,⁶ during this diffusion process, the Fe atoms in the substrate were replaced by Mg atoms by means of a "kickout" mechanism. This process created, in the upper part of the substrate, a thick (up to ≈ 30 μ m) layer of InP, beneath the epitaxially deposited Mg-InP, in which the Mg concentration was uniform at the level of the original Fe concentration ($\approx 10^{17}$ cm⁻³). By etching the heavily Mg-doped epitaxial layer as well as the adjacent region of the substrate in which the Mg concentration was still nonuniform, samples consisting of a uniformly Mg-doped layer on a Fe-doped substrate were obtained. Two samples prepared in this manner (Mg-doped sample Nos. 1 and 2) were used for the Hall transport measurements.

Figure 1 shows the secondary-ion-mass-spectrometry

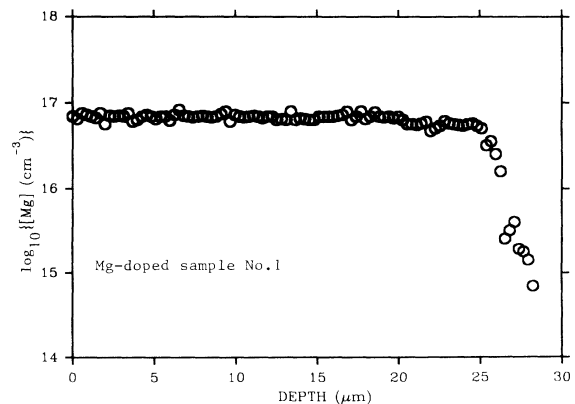


FIG. 1. SIMS depth profile of Mg-doped sample No. 1.

TABLE I. Parameters extracted from the high-temperature data.

Sample	N_A (cm^{-3})	N_D (cm^{-3})	E_A (meV)	K	a (\AA)	t (μm)	Dopant
Cd-doped sample No. 1	3.0×10^{16}	5.0×10^{15}	51.0	0.167	28.97	1.1	Cd
Cd-doped sample No. 2	5.2×10^{17}	2.7×10^{16}	39.0	0.052	33.13	1.1	Cd
Mg-doped sample No. 1	4.4×10^{16}	2.8×10^{15}	38.7	0.065	33.26	26.0	Mg
Mg-doped sample No. 2	5.2×10^{16}	3.0×10^{15}	38.3	0.058	33.43	20.0	Mg

(SIMS) profile of the Mg concentration [Mg] of Mg-doped sample No 1. [Mg] is uniform at a level of $7 \times 10^{16} \text{ cm}^{-3}$. The corresponding SIMS profile of Mg-doped sample No. 2 gave [Mg] = $1 \times 10^{17} \text{ cm}^{-3}$. The thickness t of all samples is reported in Table I.

We refer to earlier publications for details concerning the data acquisition system⁷ used in the experiments, the preparation of the samples for Hall transport measurements,⁸ verification of the uniformity of the samples,¹ and the experimental Hall measurement procedure.⁸

III. THE HIGH-TEMPERATURE REGION

In the case of extended-state conduction, for a lightly doped p -type semiconductor, the temperature (T) variation of the total hole concentration p is given by the expression⁹

$$p = \frac{1}{2} \left\{ -(N_D + N_V) + [(N_D + N_V)^2 + 4N_V(N_A - N_D)]^{1/2} \right\}, \quad (1)$$

where

$$N_V = 2(2\pi m^* k_B T / h^2)^{3/2} \beta \exp(-E_A / k_B T),$$

and $\beta = \frac{1}{4}$ is the degeneracy factor of the acceptor level, k_B the Boltzmann constant, h the Planck constant, and m^* the density-of-states effective mass. When those quantities are known, Eq. (1) is a function of only the binding energy E_A , the acceptor concentration N_A , and the residual donor concentration N_D .

The valence-band structure of InP consists of a light-hole band (LH) and a heavy-hole band (HH).¹⁰ The total drift mobility μ of p -type InP is the average of the drift mobilities of the two valence bands over the corresponding hole concentrations:⁸

$$\mu = (p_{\text{LH}}\mu_{\text{LH}} + p_{\text{HH}}\mu_{\text{HH}}) / (p_{\text{LH}} + p_{\text{HH}}). \quad (2)$$

μ_{LH} and μ_{HH} are, respectively, the mobility of the light and heavy holes, and p_{LH} and p_{HH} are their respective concentrations.

The computation of μ_{LH} and μ_{HH} was performed using a model presented in detail and discussed earlier,⁸ which takes into account interband and intraband transitions. This theory uses the relaxation times associated with the scattering mechanisms present in semiconductors, and provided a good simultaneous description of the temperature dependences of both the total free-hole concentration and the mobility of lightly doped p -type InP. With values of the physical parameters of InP previously quot-

ed,⁹ μ_{LH} and μ_{HH} , in Eq. (2), are functions of only E_A , N_A , and N_D . p_{LH} and p_{HH} , in Eq. (2), are simple analytical functions of p . Consequently, both p and μ are functions of E_A , N_A , and N_D .

The slopes of $\ln(p)$ as a function of $1/T$ in the low-temperature linear region yield the binding energy E_A of the samples when $p < N_D < N_A$. Linearity was observed in the temperature range of 29–67 K for Cd-doped sample No. 1 and 50–187 K for Cd-doped sample No. 2. This shows that excitation to the valence bands occurs at higher temperature for Cd-doped sample No. 2 than for Cd-doped sample No. 1, and indicates that the former sample is the more heavily doped. In the case of both Mg-doped samples, linearity was observed in the temperature range 38–80 K. For all four samples, the values of E_A are reported in Table I. The value $E_A = 51$ meV obtained for Cd-doped sample No. 1 is close to the value of the binding energy of Cd in InP ($E_A = 56$ meV) recently obtained by optical measurements.¹¹ For Cd-doped sample No. 2, the value $E_A = 39$ meV is significantly lower, as expected for a higher doping level.¹ The values of E_A obtained for Mg-doped sample Nos. 1 and 2 (≈ 39 meV) are also consistent with available photoluminescence results ($E_A \approx 40$ –41 meV).^{12,13}

Figure 2 shows $p(T)$ and $\mu(T)$ for both Cd-doped samples in the temperature range of 30–300 K. Figure 3 shows the corresponding results for Mg-doped sample No. 1. Mg-doped sample No. 2 yielded results similar to Mg-doped sample No. 1; the Hall data for this sample have already been published.¹⁴

The fitting procedure of theory to $\mu(T)$ and $p(T)$ of

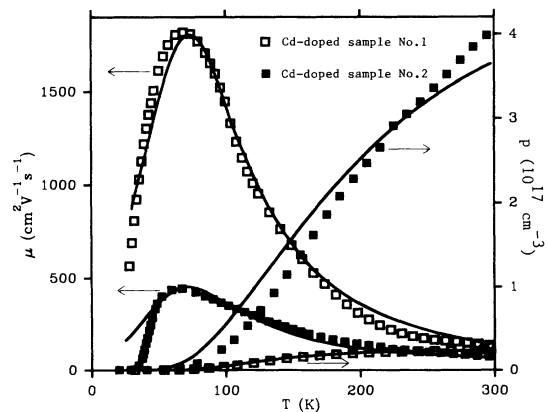


FIG. 2. Mobility and free-hole concentration of Cd-doped sample Nos. 1 and 2. The solid lines correspond to theory.

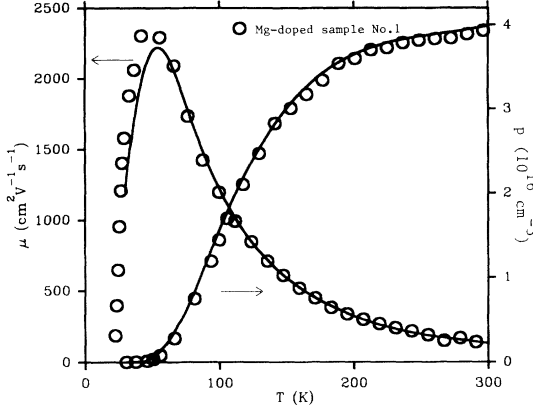


FIG. 3. Variation of the mobility and the free-hole concentration of Mg-doped sample No. 1 as a function of temperature. The solid lines correspond to theory.

lightly doped samples, which allows the determination of N_A and N_D , has been described in detail in a previous paper⁸ and was carried out for Cd-doped sample No. 1 and Mg-doped sample Nos. 1 and 2. The solid lines of Figs. 2 and 3 were computed with the values of E_A , N_A , and N_D which were obtained using this procedure for these samples and are reported in Table I. The simultaneous fits to the total hole concentration and to the mobility are excellent, which is consistent with results obtained earlier for p -type InP samples lightly doped with Zn, for which r_H was found close to 1 in the whole temperature range.⁸

For Cd-doped sample No. 2, which is more heavily doped, this fitting procedure could not be used, probably due to variations of the Hall factor r_H . An approximate simultaneous fit to the mobility and the free-carrier concentration could nevertheless be obtained as follows. With $E_A = 39$ meV and arbitrary values of N_A and N_D , the difference $\delta = N_A - N_D$ was varied until agreement was reached between theory and the experimental value of p at 300 K. N_A and N_D were then simultaneously varied, with δ held constant, until agreement was obtained between theory and the experimental μ at 78 K. Small final adjustments led to the values of N_A and N_D quoted in Table I for this sample. Fair agreement between theory and experiment has resulted from the fitting procedure for both $p(T)$ and $\mu(T)$ for Cd-doped sample No. 2, but the error is significantly larger than for the more lightly doped samples. The theoretical mobility of this sample is well above experiment below 50 K. This kind of discrepancy has been observed in n -type InP, and was attributed to the effects of impurity conduction.¹⁵ It is not present in the lower doped samples. Despite a reduced binding energy, Cd-doped sample No. 2 does not show the high-temperature flattening of $p(T)$ observed for the other samples. This shows that for high doping levels, there is still free-hole excitation to the valence bands at room temperature, where $p < N_A - N_D$. The compensation ratios $K = N_D / N_A$ reported in Table I are relatively small and decrease with increasing doping level. Table I shows a significant increase of the residual

donor concentration N_D with N_A , which is consistent with previous observations in Zn-doped InP.⁸ The origin of this effect remains uncertain.

IV. THE LOW-TEMPERATURE REGION

In lightly doped material, at sufficiently low temperature, electrical transport is by means of variable-range hopping. The conductivity is generally of the form¹⁶

$$\sigma = \Gamma_0 T^{-1/2} \exp[-(T_0/T)^s], \quad s = \frac{1}{4}, \quad (3)$$

where¹⁷

$$T_0 = 49 / (K_B D_0 a^3) \quad (4)$$

and

$$a = h / [2\pi(2m^* E_A)^{1/2}]. \quad (5)$$

h is the Planck constant and $m_{LH}^* = 0.089$ a.u. is the effective mass of the light holes⁸ (although this value is the most frequently used in the literature, a value $m_{LH}^* = 0.08$ a.u. is sometimes quoted). Equation (3) was derived by Mott by assuming a constant density of states D_0 in the impurity band at the position of the Fermi level (E_F).

At higher temperatures, a range is generally found where conduction is by nearest-neighbor hopping, with a conductivity of the form¹⁸

$$\sigma = \Gamma_3 T^{-1} \exp(-T_3/T), \quad (6)$$

where

$$\Gamma_3 = \beta_3 T_3 a^{-3} (N_A^{1/3} a)^{-0.15} \exp[-\alpha / (N_A^{1/3} a)] \quad (7)$$

and

$$T_3 = 0.61 T_D. \quad (8)$$

T_D is the temperature corresponding to the energy of the Coulomb interaction at the average distance between majority impurities, and is given by¹⁷

$$T_D = (4\pi/3)^{1/3} q^2 N_A^{1/3} / (K_B \kappa). \quad (9)$$

β_3 is a constant, q the electronic charge, and κ the low-frequency dielectric constant [12.35 for InP (Ref. 8)]. α has a theoretical value of 1.73.²

Shklovskii and Yanchev³ considered the saturation of the nearest-neighbor hopping mechanism in the case of low compensation. This situation, expected in an almost full impurity band, occurs when the concentration of the charge carriers allowed to hop reaches the density of available sites, which is equal to the concentration of compensating impurities. An estimate of the temperature at which this becomes important is²

$$T_s = T_3 / \ln(N_A / N_D). \quad (10)$$

The solution of an appropriate neutrality equation leads to a conductivity of the form

$$\sigma = \Gamma_3 T^{-1} \exp[-T_D / (TX)], \quad (11)$$

where X is the solution of the equation

$$N_D \exp(-X^3) = 7.14 \times 10^{-4} X^6 + N_A \exp[-T_D/(TX)]. \quad (12)$$

Figure 4 shows a plot of $\ln(\sigma T)$ as a function of $1/T$ for both Cd-doped samples. For Cd-doped sample No. 1, a linear behavior is observed in the temperature range of 15–25 K. Above 25 K, the fast increase of σ observed for this sample is due to free-hole excitation to the valence bands, which corresponds to the variation of $p(T)$ shown in Fig. 2. For Cd-doped sample No. 2, linearity of $\ln(\sigma T)$ as a function of $1/T$ is observed in the temperature range of 10–34 K. This broader temperature range is expected for more heavily doped samples, where impurity band conduction is stronger. The conductivity of the two samples is well described by Eq. (6), which corresponds to nearest-neighbor hopping. Equation (6) was fitted to the conductivity of the samples with an iterative least-squares technique. For both samples, Γ_3 and T_3 were unconstrained, and the resulting values, quoted in Table II, were used to generate the solid lines of Fig. 4. The values of a given by Eq. (5) are reported in Table I. The values of T_3 (extracted from the nearest-neighbor hopping regime), and the values of T_D , as calculated with Eq. (8), are quoted in Table II. With the values of N_A given in Table I, Eqs. (8) and (9) provided the theoretical values of T_3 that are reported in Table II. Despite very different acceptor concentrations, the samples have similar values of T_3 , corresponding to similar widths of their impurity bands.² This can be explained by the fact that Cd-doped sample No. 2 has very low compensation, and a correspondingly low level of disorder. For T_3 , the discrepancy between theory and experiment is in all cases of the order of 40%, which is a reasonable result.²

The theoretical value of $a = 1.73$, in Eq. (7), can be tested with the data extracted from the nearest-neighbor hopping regime of the two Cd-doped samples. If we define

$$y = \Gamma_3 a^3 (N_A^{1/3} a)^{0.15} / T_3, \quad (13)$$

a plot of $\ln(y)$ as a function of $x = 1/(N_A^{1/3} a)$ should, according to theory, yield a straight line with slope $-\alpha$. The values of x and y obtained for each sample are quoted in Table II. From those values, we obtain $\alpha = 1.297$. This result, which is sensitive to m_{LH}^* , is 25% lower than the corresponding theoretical prediction. The value $m_{LH}^* = 0.08$ a.u. would increase α by about 5%.

Figure 5 shows a plot of $\ln(\sigma T)$ as a function of $1/T$ for Mg-doped sample No. 1. The dashed-double-dotted line is a fit of Eq. (6) to the data in the range 4.3–10 K,

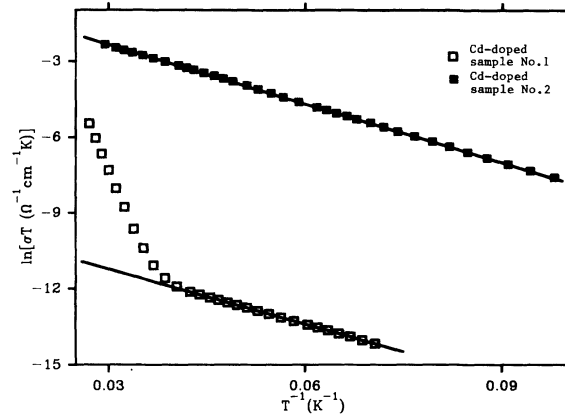


FIG. 4. $\ln(\sigma T)$ as a function of $1/T$ for Cd-doped sample Nos. 1 and 2. Nearest-neighbor hopping is observed for Cd-doped sample No. 1 in the range of 15–25 K. For this sample, excitation to the valence bands occurs above 25 K. The conductivity of Cd-doped sample No. 2, which is more heavily doped, shows nearest-neighbor hopping in the range 10–34 K. The solid lines correspond to the theoretical model discussed in the text with the parameters quoted in Table II.

generated with $\Gamma_3 = 1.339 \times 10^{-3} \Omega^{-1} \text{cm}^{-1} \text{K}$ and $T_3 = 33.36$ K. The deviation of the experimental points from the dashed-double-dotted line observed above 10 K has been predicted by Shklovskii and Yanchev,³ and attributed to the saturation of the nearest-neighbor hopping regime in the case of low compensation. $\sigma(T)$ should in such a case be described by Eq. (11), where X is the solution of Eq. (12). This equation can be solved numerically with the values of N_A and N_D displayed in Table I, and with T_D , as calculated with Eq. (8) and the experimental value of T_3 . The dashed-dotted line of Fig. 5 is the result of the computation with the value of Γ_3 quoted above. Although, as predicted by the model,³ all lines merge at $T \approx 2$ K (not shown in the figure), a large discrepancy is observed between theory and experiment. The onset of the deviation of the experimental points from the straight line occurs at a temperature higher ($T \approx 10$ K) than predicted by the model and is more abrupt. This result is very similar to our previous observations in low compensation Zn-doped epitaxial layers grown by MOCVD.¹

Figure 6 shows the nearest-neighbor hopping conductivity of Mg-doped sample No. 2. The lines have the same meaning as for Mg-doped sample No. 1, and confirm the previous observations. In this case, we obtained $T_3 = 32.43$ K and $\Gamma_3 = 7.21 \times 10^{-4} \Omega^{-1} \text{cm}^{-1} \text{K}$

TABLE II. Parameters corresponding to nearest-neighbor hopping.

Sample	Γ_3 ($\Omega^{-1} \text{cm}^{-1} \text{K}$)	T_3 (expt.) (K)	T_3 (theor.) (K)	$1/(N_A^{1/3} a)$	T_D (expt.) (K)	y ($\Omega^{-1} \text{cm}^2$)
Cd-doped sample No. 1	1.172×10^{-4}	72.36	41.40	11.11	118.62	2.744×10^{-26}
Cd-doped sample No. 2	9.932×10^{-1}	77.98	107.2	3.754	127.84	3.798×10^{-22}
Mg-doped sample No. 1	7.501×10^{-3}	41.50	47.04		68.03	
Mg-doped sample No. 2	3.950×10^{-3}	40.25	49.73		65.98	

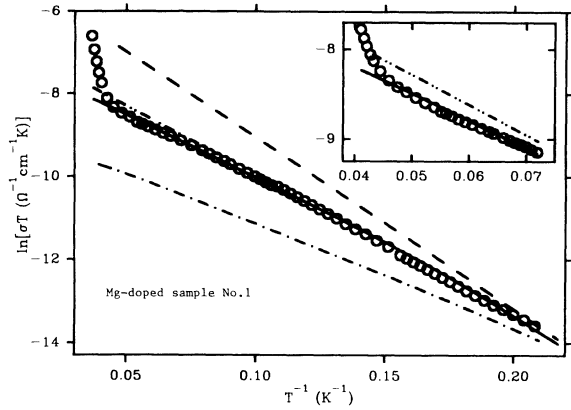


FIG. 5. $\ln(\sigma T)$ as a function of $1/T$ for Mg-doped sample No. 1. The dashed-double-dotted line is the fit of Eq. (6) to the linear region of the data. The dashed-dotted line represents the corresponding saturated regime. The solid line is the fit of Eq. (11) to σ , and the dashed line shows the corresponding unsaturated regime. The inset is an enlargement of the figure at the onset of excitation to the valence band.

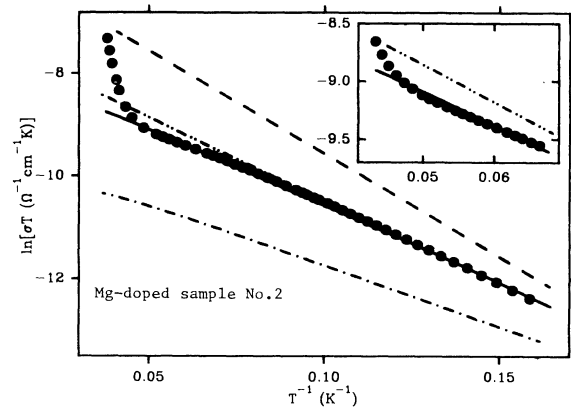


FIG. 6. $\ln(\sigma T)$ as a function of $1/T$ for Mg-doped sample No. 2. The dashed-double-dotted line is the fit of Eq. (6) to the linear region of σ . The dashed-dotted line represents the corresponding saturated regime. The solid line is the fit of Eq. (11) to σ , and the dashed line shows the corresponding unsaturated regime. The inset is an enlargement of the figure at the onset of excitation to the valence band.

from a fit of Eq. (6) to the linear region of σ . The value of T_3 corresponding to Mg-doped sample No. 2 is slightly lower than the one obtained for Mg-doped sample No. 1, which is more lightly doped. Since T_3 is expected to increase with doping, this result appears to be anomalous. However, this small discrepancy may be attributed to the experimental error or to the somewhat different compensation levels of the samples. The theoretical values of T_3 are reported in Table III. A discrepancy of the order of 50% is observed for both samples.

Although this treatment, as suggested by Shklovskii and Yanchev,³ provides qualitative agreement between experiment and theory, a different interpretation of the data corresponding to the saturation of the nearest-neighbor hopping conductivity of Mg-doped sample Nos. 1 and 2 gives a much better result. The dashed-dotted lines of Figs. 5 and 6, which correspond to the theoretical saturation of the nearest hopping regime, show a linear region from 6 to 12 K, approximately. This suggests that the low- T region of the nearest-neighbor hopping conductivity of Mg-doped sample Nos. 1 and 2 may be interpreted as a region where saturation has already occurred, and may be described by Eq. (11) instead of Eq. (6). As N_A and N_D are previously determined quantities, and with X given as the solution of Eq. (12), σ in Eq. (11) is a function of only Γ_3 and T_D . Consequently, both σ and

its partial derivatives with respect to Γ_3 and T_D can be numerically calculated for any (Γ_3, T_D) . Equation (11) can then be fitted to the nearest-neighbor hopping data of Mg-doped sample Nos. 1 and 2 with Γ_3 and T_D as adjustable parameters. The fits have been performed with a limited number of experimental points, and the results are reported in Table II. Compared with the earlier treatment, a much better agreement between theory and experiment is obtained for T_3 , with a discrepancy of only 12% for Mg-doped sample No. 1 and 19% for Mg-doped sample No. 2. The solid lines of Figs. 5 and 6 were generated with Eq. (11) and the results of the fits, and show excellent agreement between theory and experiment in the whole nearest-neighbor hopping regime for both samples. The dashed lines, which were generated with Eq. (6) and Γ_3 and T_3 as given in Table II, describe the corresponding unsaturated regimes. As expected by theory, the solid and dashed lines merge around 2 K (not shown).

The fact that saturation of the nearest-neighbor hopping regime is not observed for the Cd-doped samples is consistent with the values of T_s reported in Table III. In the case of those samples, due to higher doping level or to larger compensation, there is excitation to the valence band before saturation becomes possible.

Due to the high resistivity of Cd-doped sample No. 1, its conductivity could not be accurately determined at

TABLE III. Parameters corresponding to variable-range hopping.

Sample	Γ_0 ($\Omega^{-1} \text{ cm}^{-1} \text{ K}^{1/2}$)	T_0 (expt.) (K)	s	D_0 ($\text{erg}^{-1} \text{ cm}^{-3}$)	T_0 (theor.) (K)	T_s (K)
Cd-doped sample No. 1						40.43
Cd-doped sample No. 2	5.34×10^9	5.70×10^6	0.259	1.47×10^{31}	6.63×10^5	26.37
Mg-doped sample No. 1	2.21×10^8	1.38×10^7	0.236	3.55×10^{30}	2.72×10^6	15.18
Mg-doped sample No. 2	1.47×10^4	1.58×10^6	0.251	4.34×10^{30}	2.19×10^6	14.14

temperatures below approximately 15 K. For Cd-doped sample No. 2, accurate measurements could be performed down to $T=7.4$ K (below that temperature, low-electric-field conditions could not be maintained, as non-linearity of the I - V characteristics measured across the contacts of the sample started to develop). A clear deviation from the nearest-neighbor hopping regime was observed for this sample in the temperature range 7.4–9.5 K, and the corresponding data for σ are shown in Fig. 7. Equation (3) was fitted to the data with Γ_0 , T_0 , and s as adjustable parameters. The results are reported in Table III. The corresponding solid line of Fig. 7 for Cd-doped sample No. 2 was generated with Eq. (3) and those parameters. Mott's law is in excellent agreement with the data. Although the temperature range where it is observed is relatively small, the number of experimental points is large, and the corresponding variation of σ is of the order of two decades. The average relative error of the fit is 2.3×10^{-3} . Equation (4) gives the theoretical prediction for T_0 . There, a has already been calculated and is quoted in Table I. By assuming a flat density of states in the impurity band, a rough estimate¹ of D_0 at E_F is

$$D_0 = N_A / (2K_B T_D). \quad (14)$$

The values of D_0 and T_0 are reported in Table III. The experimental value of T_0 is about a factor of 8 larger than the theoretical prediction. A more realistic shape for the density of states of the impurity band would modify this result.

Figure 7 also shows the conductivity of Mg-doped sample Nos. 1 and 2 in the temperature range of approximately 3.1–6.3 K. Mott's variable-range hopping is observed in both cases. The solid lines are fits of Eq. (3) to the data, with Γ_0 , T_0 , and s as free parameters. The corresponding experimental values are reported in Table III. The power s is again consistent with Mott's theory. For Mg-doped sample No. 1, theory is approximately a factor of 5 above experiment. Nevertheless, we point out that when we take $s = \frac{1}{4}$ in Eq. (3) with the two other parameters left free to vary, the corresponding fit to the conduc-

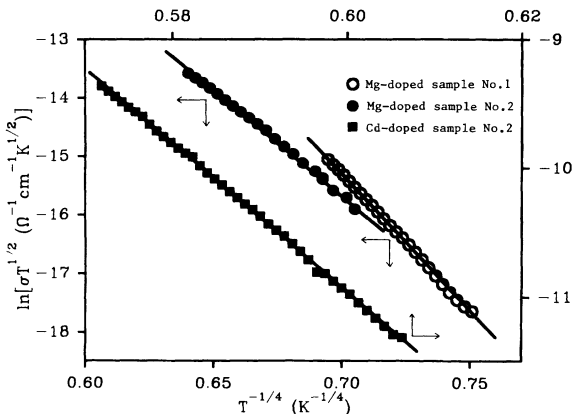


FIG. 7. $\ln(\sigma T^{1/2})$ as function of $T^{-1/4}$ for three samples. Mott's variable-range hopping is observed, and the solid lines correspond to the results of the theoretical model discussed in the text.

tivity of Mg-doped sample No. 1 provides an experimental value of T_0 that is only 30% below theory. For Mg-doped sample No. 2, experiment is slightly above theory. Those results can be considered excellent in comparison with the large experimental underestimate obtained when the temperature dependence of the prefactor of Mott's expression for the conductivity is not taken into account.¹⁷

Figure 8 shows the variation with temperature of the Hall coefficient R_H of the same three samples in the range 10–50 K. The peak observed at $T=26$ K for the Mg-doped samples and at $T=45$ K for Cd-doped sample No. 2 is well known to be due to two-band conduction,¹⁵ and occurs at higher T with increasing doping level. An unusual feature of the data for both Mg samples is the sign reversal of R_H observed at approximately $T=22$ K, which corresponds to the onset of impurity conduction, as shown in Figs. 5 and 6. The relatively flat behavior of R_H observed between 13 and 20 K corresponds to the saturation of the nearest-neighbor hopping regime, and could be consistent with a stabilization of the concentration of the mobile carriers with increasing temperature. Similar behavior has been observed in Zn-doped InP,¹ but without the feature of a sign reversal of R_H . Below 13 K, a fast decrease of R_H is observed, which could indicate a decrease of the concentration of the mobile carriers.

The sign reversal of R_H obtained with these Mg-diffused substrates has not been observed in detailed Hall transport measurements performed on low-compensation Zn¹-doped epitaxial layers of InP grown by MOCVD, and does not appear in the Cd-doped material. A sign reversal of R_H has been observed in the strong localization regime of III - V compounds,¹⁹ and linked to conduction in a nearly full impurity band (low compensation). The sign of the Hall coefficient in hopping conduction has been considered by Emin,²⁰ who concludes that it may depend on the local geometry and on the nature and orientation of the local electronic states. This suggests the possibility that there are differences between the local environments of acceptor species that have been diffused into InP from an external source and have stopped at stable substitutional sites by means of a "kickout" mecha-

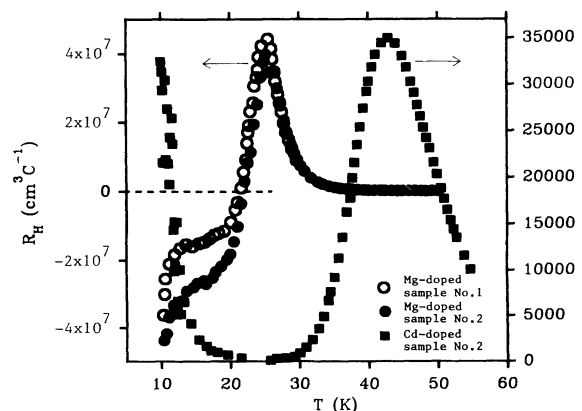


FIG. 8. Low-temperature Hall factor of three samples. A sign reversal of R_H is observed in the Mg-doped samples.

nism,⁶ and of acceptor species that have been directly incorporated during epitaxial growth. Differences have been observed in the compensation ratio K . In samples prepared with dopant diffusion from an external source into Fe-doped InP substrates, K was found to be approximately 0.05, both in the case of Mg (see Table I) and Zn.²¹ In samples doped at similar levels ($N_A \approx 10^{17} \text{ cm}^{-3}$) during epitaxy, K was found to be approximately 0.2, both for Zn (Ref. 1) and Cd (see Cd-doped sample No. 2) doping. One may speculate that differences in the concentrations and distributions of vacancies and interstitials associated with the two methods of layer fabrication may be responsible for the differences in electrical characteristics.

V. CONCLUSIONS

In conclusion, we have reported on the electrical properties of p -type InP layers in which Cd and Mg are the dopant species. In the purest samples, the binding energy was found to be $E_A = 51$ and 38.7 meV for Cd- and Mg-doped layers, respectively. These results are consistent with recent optical measurements of similarly doped InP layers, as reported in the literature. As expected, when the Mott transition is approached, the binding energy decreases with increasing doping level.

The impurity concentrations of the samples were deter-

mined with an electrical transport model. The theory provided a good simultaneous description of the free-hole concentration and the mobility in the temperature range 30–300 K. For high-purity InP, the Hall factor r_H appeared to be close to 1 and independent of the temperature in this temperature range.

Nearest-neighbor hopping was observed in all samples. A model by Shklovskii and Efros provided an excellent description of the data, and consistency with the activation energies of the layers. Due to their low doping and compensation levels, saturation of the conductivity with increasing temperature was only observed in the Mg-doped samples, and found to be in excellent agreement, with an appropriate interpretation of the data, with a model by Shklovskii and Yanchev based on the saturation, with increasing temperature, of unoccupied impurity sites available to the hopping carriers. At lower temperatures, Mott's variable-range hopping was observed, and was found to be consistent with theory.

A reversal of the sign of the Hall coefficient was observed at the onset of the strong localization regime of the Mg-doped samples, which was not present in the Cd-doped layers. It is suggested that this sign reversal may be due to differences in the local crystallographic environment of the acceptors in the two types of material, resulting from the different fabrication techniques used to obtain the Cd- and Mg-doped InP layers.

-
- ¹M. Benzaquen, B. Belache, and C. Blaauw, *Phys. Rev. B* **41**, 12 582 (1990).
- ²B. I. Shklovskii and A. L. Efros, in *Electronic Properties of Doped Semiconductors*, edited by M. Cardona, P. Fulde, and H. J. Queisser (Springer-Verlag, Berlin, 1984).
- ³B. I. Shklovskii and I. Y. Yanchev, *Fiz. Tekh. Poluprovodn.* **6**, 1616 (1972) [*Sov. Phys.—Semicond.* **6**, 1395 (1973)].
- ⁴C. Blaauw, B. Emmerstorfer, and A. J. SpringThorpe, *J. Cryst. Growth* **84**, 431 (1987).
- ⁵C. Blaauw, R. A. Bruce, C. J. Miner, A. J. Howard, B. Emmerstorfer, and A. J. SpringThorpe, *J. Electron. Mater.* **18**, 567 (1989).
- ⁶C. Blaauw, B. Emmerstorfer, R. A. Bruce, and M. Benzaquen, in *Semi-Insulating III-V Materials*, Proceedings of the 6th Conference, Toronto, 1990, edited by A. Milnes and C. J. Miner, IOP Conf. Proc. (Institute of Physics and Physical Society, Bristol, 1990), p. 137.
- ⁷P. Weissfloch, M. Benzaquen, and D. Walsh, *Rev. Sci. Instrum.* **58**, 1749 (1987).
- ⁸M. Benzaquen, B. Belache, C. Blaauw, and R. A. Bruce, *J. Appl. Phys.* **68**, 1694 (1990).
- ⁹J. S. Blakemore, *Semiconductor Statistics* (Pergamon, Oxford, 1962), p. 134.
- ¹⁰J. D. Wiley, in *Semiconductors and Semimetals*, edited by R. K. Willardson and A. C. Beer (Academic, New York, 1975), Vol. 10.
- ¹¹S. Banerjee, A. K. Srivastava, B. M. Arora, J. W. Sulhoff, and J. L. Zyskind, *Appl. Phys. Lett.* **53**, 1429 (1988).
- ¹²E. Kubota, Y. Ohmori, and K. Sugii, *J. Appl. Phys.* **55**, 3779 (1984).
- ¹³B. J. Skromme, G. E. Stillman, J. D. Oberstar, and S. S. Chan, *Appl. Phys. Lett.* **44**, 319 (1984).
- ¹⁴M. Benzaquen, B. Belache, and D. Walsh, *Phys. Rev. B* **44**, 13 205 (1991).
- ¹⁵M. Benzaquen, M. Beaudoin, D. Walsh, and N. Puetz, *Phys. Rev. B* **38**, 7824 (1988).
- ¹⁶N. F. Mott, *Philos. Mag.* **19**, 835 (1969).
- ¹⁷R. Mansfield, in *Hopping Transport in Solids*, edited M. Pollak and B. I. Shklovskii (Elsevier, Amsterdam, 1988).
- ¹⁸B. I. Shklovskii, *Fiz. Tekh. Poluprovodn.* **6**, 1197 (1972) [*Sov. Phys.—Semicond.* **6**, 1053 (1972)].
- ¹⁹M. Benzaquen, D. Walsh, and K. Mazuruk, *Solid State Commun.* **61**, 803 (1987).
- ²⁰D. Emin, *Philos. Mag.* **35**, 1189 (1977).
- ²¹M. Benzaquen (unpublished).